Aggregation of DNA Enhanced by the Protoberberine Alkaloids, Coralyne and Berberine

Zenei TAIRA,*[,a] Mitsuhiro MATSUMOTO,[b] Shiro ISHIDA,[a] Tsutomu ICHIKAWA,[a] and Yoko SAKIYA[a]

Faculty of Pharmaceutical Sciences, Tokushima Bunri University,[a] Tokushima 770, Japan, and Faculty of Integrated Arts and Sciences, University of Tokushima,[b] Tokushima 770, Japan.

Received December 15, 1993; accepted April 11, 1994

The aggregation of DNA caused by coralyne was studied by spectroscopic, viscosity and electric birefringence measurements. Aggregation was markedly enhanced over a narrow range of coralyne to DNA phosphate ratio and then followed by precipitation. The electric birefringence measurements indicated that the ratio at the maximal aggregation varied depending on the concentration of coralyne, finally reaching 1 : 1 at higher concentrations. The particles (type I) for such enhanced aggregation were estimated to be prolate ellipsoids 1700—4000 Å in length with a diameter of 1400—4000 Å. At higher coralyne concentrations, another particle (type II) was formed which was a thick rod-like particle 1700—4000 Å in length with a diameter of 120—210 Å. These dimensions indicate that type I and II particles consist respectively of several tens of thousands and some hundreds of molecules of DNA.

On the other hand, berberine did not produce such a marked aggregation of DNA, and the result was a thick rod-like particle 1700—4000 Å in length with a diameter of 300—1000 Å. The enhancement by coralyne and berberine is discussed in terms of intermolecular interactions.

Keywords DNA; coralyne; berberine; aggregation; intercalation; electric birefringence

Protoberberine alkaloids (Fig. 1), such as coralyne and berberine, exhibit a wide variety of pharmacological and biological activities,[1,2] including antimicrobial, antitumor, antileukemic and antineoplastic properties. Coralyne is effective against both L1210 lymphoid and P388 lymphocytic leukemias,[1] and is also able to inhibit enzymes[2] such as transfer RNA methyltransferase and the reverse transcriptase activity of RNA tumor viruses. Furthermore, the fused planar cationic aromatic ring system of coralyne is potentially capable of intercalation[3-5] with DNA in a manner analogous to daunorubicin, ethidium bromide, *etc.* Zee-Cheng and Cheng[5a] have investigated the effect of coralyne on the viscosity of DNA solutions and found that at lower molar ratios of coralyne to DNA, coralyne can form an intercalated complex with DNA, and that, as the molar ratio increases, it forms DNA-induced aggregation, which takes place along the deoxyribose phosphate backbone. The aggregation of dyestuffs such as acridine orange[6] produced by DNA has been studied for a long time. Bradley and Felsenfeld[6a] have developed a model to interpret it and Zee-Cheng and Cheng[5a] have explained the aggregation of DNA by coralyne using this model. Wilson *et al.*[5b] have shown that the intercalation of coralyne with DNA may play a critical role in its antileukemic action, because coralyne removes and reverses the supercoiling of bacteriophage PM-2 DNA. Over a decade ago, berberine was reported to exhibit a variety of biological effects,[7] such as antibacterial and antiprotozoal activities, and its physicochemical properties[7] have been investigated. Although berberine possesses partial saturation in ring B in contrast to the planar coralyne molecule, Davidson *et al.*[7a] have shown that berberine binds to DNA by intercalation and its aggregation ability is enhanced by the addition of DNA. Therefore, it is of interest how this steric factor influences its interaction with DNA. The aggregation often accompanies large changes in the electrical and hydrodynamic properties of the solution. Therefore, electric birefringence should serve as a powerful method for studying the nature of the aggregation. We report here the aggregation of DNA caused by coralyne and berberine and discuss whether this is related to their interaction with DNA.

Experimental

Materials Salmon sperm DNA was purchased from Wako Pure Chemical Industries, Ltd., Japan, calf thymus DNA from Pharmacia Fine Chemicals and from Tokyo Chemical Industry Co., Ltd., Japan, and cod sperm DNA from Tokyo Chemical Industry Co., Ltd., Japan. The other compounds such as coralyne · HCl · H_2O and berberine · HCl, were of commercially available analytical grade. These were used without further purification.

Viscosity Viscosities were measured using a modified Ubbelohde viscometer at 25.00±0.01 °C. The DNA solutions, 0.1 mg/ml in 50 mM Tris–HCl buffer (pH 7.6) containing 50 mM KCl, were titrated with buffer.

Spectral Measurements Ultraviolet (UV) and visible spectra were measured on a Shimadzu M300 spectrophotometer in a 10 mm light-path cell. Circular dichroism (CD) spectra were recorded on a JASCO J-500 spectropolarimeter in a 1 mm light-path cell at room temperature. The DNA phosphate concentrations of the solutions were determined by the method of Fiske–Subbarow[8a] as modified by Chen *et al.*[8b]

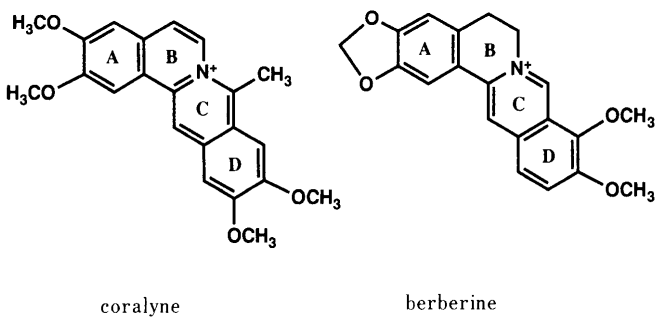

coralyne berberine

Fig. 1. The Chemical Structures of Coralyne and Berberine

Electric Birefringence The electric birefringence was measured using an instrument equipped with an He–Ne laser (wavelength $\lambda = 632.8$ nm) with a power of 2 mW at 25 °C. The light was polarized by a Glan–Thompson prism in a plane at 45° with respect to the direction of the applied field. All samples were dissolved in a buffer consisting of 0.5 mM Na_2HPO_4, 1 mM NaH_2PO_4 and 0.25 mM Na_2EDTA, pH 6.55, and transferred to a 10 mm path-length quartz spectrophotometer cell, in which two platinum electrodes supported by a 3.03 mm Teflon spacer were placed. The photodetector employed was a Hamamatsu R1104 photomultiplier, and a pre-amplifier produced the output voltage. The output signal was converted to a digital signal using a Kawasaki MR-50E digitizer and analyzed using an NEC PC9801 personal computer.

Analysis of Electric Birefringence When a DNA solution is placed in an electric field, the DNA molecules, anionic polymers, are oriented in the direction of the electric field. Electric birefringence $\Delta n = n_{//} - n_{\perp}$ can then be observed in the solution, where $n_{//}$ and $n_{\perp}$ are the refractive indices parallel and perpendicular to the electric field, respectively. When a square-wave electric pulse is applied to the solution, the DNA molecules should orient themselves in response to the electric field, and the birefringence Δn can then be measured for the rising, steady-state and decay phases of the orientation. From these measurements, a birefringence–decay curve for the orientation, after removing the electric field, can provide useful information about a multi-dispersion system. The birefringence is defined by Eq. 1.

$$\Delta n(t) = \sum_{i=1}^{N} \Delta n_i(0) \cdot \exp(-6\Theta_i t) \tag{1}$$

Where $\Delta n_i(0)$ refers to the birefringence from the i-th species at the steady-state orientation, as

$$\Delta n_i(0) = \frac{2\pi C_{vi}(g_1 - g_2)}{n} \Phi_i \tag{2}$$

denoted by Eq. 2, where $g_1 - g_2$ is the optical anisotropy factor independent of the length of the solute particle. The volume fraction, C_{vi}, of the i-th species of solute is assumed to be nearly equal to the product of the volume and the number of solute particles at lower concentrations. Therefore, it should be proportional to the length of a rod-like particle. At higher electric fields, the orientation factor Φ_i can be assumed to be unity, *i.e.*, $\Phi_i \approx 1$, because most of the molecules are oriented in the direction of the field. Therefore, the birefringence should be approximately proportional to the length of a particle, *i.e.* $\Delta n_i(0) \propto L_i$, and the rotatory diffusion constant Θ_i for the i-th species depends on the axial ratio p_i and the length L_i as follows:

$$\Theta_i = f(p_i)/L_i^3 \tag{3}$$

The function $f(p_i)$ depends on the particle shape: *e.g.*, Broersma's equation[9d] (Eq. 4) for a rigid rod, and Perrin's equation[9g] (Eq. 5) for a prolate ellipsoid ($p_i > 1$).

$$f(p_i) = \frac{3kT}{\pi\eta_0}\left[\ln 2p_i - 1.57 + 7\left(\frac{1}{\ln 2p_i} - 0.28\right)^2\right] \tag{4}$$

$$f(p_i) = \frac{3kT}{2\pi\eta_0} \cdot \frac{1}{1-p_i^4}\left[-1 + \frac{2-p_i^2}{2\sqrt{1-p_i^2}} \ln\left(\frac{1+\sqrt{1-p_i^2}}{1-\sqrt{1-p_i^2}}\right)\right] \tag{5}$$

Where η_0 is the viscosity of the solvent, k is Boltzman's constant and T the absolute temperature. The function $f(p_i)$ should be assumed to be constant in larger p_i regions. The decay curve can be analyzed in terms of the initial slope and the integration methods.[9] Since there is a relationship between the relaxation time and the diffusion constant, $6\Theta_i = 1/\tau_i$, the initial slope of the normalized decay curve and the integrated area under the normalized birefringence curve, respectively, are related to the mean reciprocal relaxation time $\langle 1/\tau \rangle_{biref}$ (Eq. 6) and the mean relaxation time $\langle \tau \rangle_{biref}$ (Eq. 7) as follows:

$$\frac{d}{dt}\left\{\frac{\Delta n(0)}{\Delta n(t)}\right\}_{t=0} = -\frac{\sum \Delta n_i(0)(6\Theta_i)}{\sum \Delta n_i(0)} = -6\langle\Theta\rangle_{biref} = -\left\langle\frac{1}{\tau}\right\rangle_{biref} \tag{6}$$

$$\int_0^{\infty} \frac{\Delta n(0)}{\Delta n(t)} dt = \frac{\sum \Delta n_i(0)\tau_i}{\sum \Delta n_i(0)} = \frac{1}{6}\left\langle\frac{1}{\Theta}\right\rangle_{biref} = \langle\tau\rangle_{biref} \tag{7}$$

If the electric field is high, both the mean values, $\langle 1/\tau \rangle_{biref}$ and $\langle \tau \rangle_{biref}$, are approximately proportional to the mean lengths $\overline{L^{-2}}/\overline{L}$ and $\overline{L^4}/\overline{L}$, respectively. Consequently, the initial slope method gives the length predominantly for smaller particles, while the integration method is for larger particles.[9g] These indicate that dispersed particles should lie between both mean values. Their product $\langle \tau \rangle_{biref}\langle 1/\tau \rangle_{biref}$ provides a measure of the polydispersity of the solute particles, due to the following:

$$\left\langle\frac{1}{t}\right\rangle_{biref} \langle\tau\rangle_{biref} = \frac{\overline{L^4} \cdot \overline{L^{-2}}}{\overline{L^2}} \tag{8}$$

On the other hand, if the electric field is low, the dispersion of particles can be estimated in terms of the Kerr constant, because the birefringence at steady-state can be presumed to be proportional to the square of the magnitude of the electric field, E, as follows:

$$\Delta n = B\lambda E^2 \tag{9}$$

Where λ is the wavelength of the light and B the Kerr constant. The specific Kerr constant (B/C), *i.e.*, the ratio of B to the solute concentration C, provides another measure of particle size.

Ultrafiltration The interaction of coralyne with DNA was determined according to a membrane filtration method using a Centrifree micropartition device MPS-1 (Amicon, no. 4103) equipped with a thin membrane (YNT) having a molecular weight cut-off of 30000. After each sample, containing 50 μg/ml DNA and various concentrations of coralyne in a standard buffer consisting of 1/15 mM Tris–HCl buffer (pH 7.6) containing 50 mM KCl, was allowed to stand for 60 min at room temperature, the mixture was transferred to the Centrifree device. Controls containing the same amounts of ligand, but no DNA, were run in parallel to determine the absorption blank due to the membrane. Centrifugation was carried out at 2000 rpm for 10 min, and the absorption coefficient of the filtrate was measured at 418 nm. The bound ligand concentration was corrected using the blank value.

Results and Discussion

Upon the addition of salmon sperm DNA to coralyne solution, a spectrum was obtained with an absorption maximum at 418 nm showing a hypochromic shift and splitting into twin peaks with maxima at 418 and 437 nm, as shown in Fig. 2. This shows that coralyne is capable of intercalation with DNA in a manner analogous to

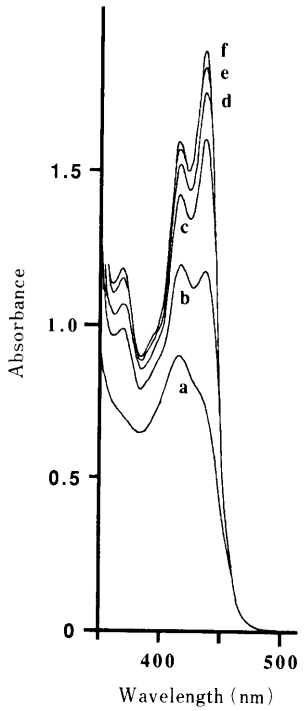

Fig. 2. Effect of DNA on the Absorption Spectra of Coralyne

Coralyne, 2×10^{-4} M; DNA phosphate/coralyne ratio: a, 0; b, 0.95; c, 3.80; d, 5.68; e, 7.57; f, 9.52.

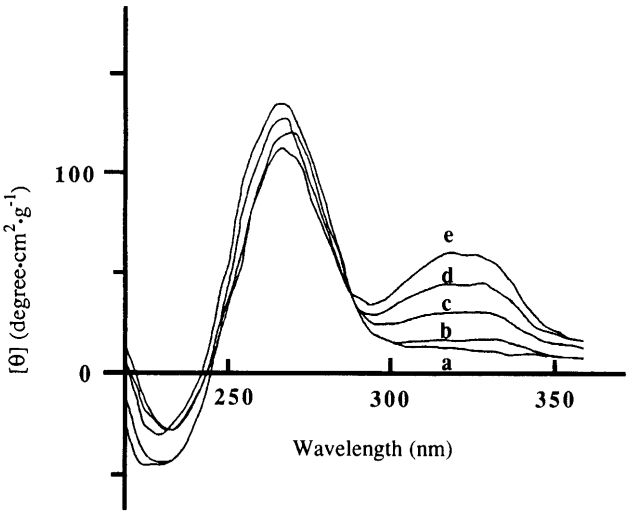

Fig. 3. Changes in the CD Spectra of DNA Solutions Produced by Coralyne

Salmon sperm DNA 600 μg/ml (DNA phosphate 1.52×10^{-3} M), coralyne: a, 0 M; b, 0.5×10^{-4} M; c, 1.25×10^{-4} M; d, 2.0×10^{-4} M; e, 3.0×10^{-4} M.

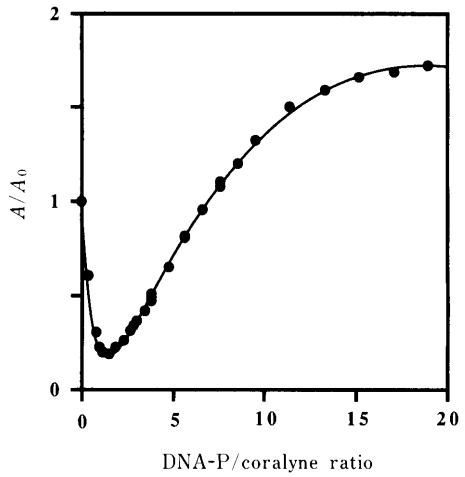

Fig. 4. Effect of DNA on the Absorption Coefficient of Coralyne at 418 nm

A denotes the absorbance of a 2.0×10^{-4} M coralyne solution in the presence of salmon sperm DNA at 418 nm and A_0 that in the absence of DNA.

ethidium bromide.[5] This was further confirmed by the appearance of an induced peak at 320 nm in the circular dichroism (CD) spectra of salmon sperm DNA solutions in the presence of coralyne, as shown in Fig. 3. In some of these solutions containing coralyne and DNA, a yellowish precipitate appeared. Figure 4 shows the changes in the absorption coefficients of those supernatants at 418 nm after the precipitates were removed by centrifuging the solutions containing 2.0×10^{-4} M coralyne and 0—30 μg/ml of DNA at 2000 rpm for 15 min. This shows that the precipitation reaches a maximum when the molar ratio of coralyne to the phosphate content of DNA (referred to as DNA-P) is near unity, *i.e.* 1 : 1. This was also confirmed by measuring the phosphate concentrations in the supernatants (data not shown). These results indicate that the aggregation occurs over a certain critical range of the molar ratio of coralyne to DNA-P. In order to determine the stoichiometric constituents of the precipitates, elementary analyses were performed after the materials were washed with water and lyophilized. Although the components varied somewhat from sample to sample, they were distinct from coralyne and DNA themselves and probably consisted of equi-molar components. The mean elementary analysis showed that the precipitate contained C 48.9%, H 4.6%, N 6.9%; salmon sperm DNA C 32.4%, H 3.9%, N 13.8%; coralyne C 66.1%, H 5.6%, N 3.5%. Unfortunately, we could not determine the exact stoichiometry of the coralyne–DNA complex. Therefore, we studied the aggregation further by means of viscosity and electric birefringence measurements.

TABLE I. The Intrinsic Viscosities, Molecular Weights and Lengths of the DNAs Studied

DNA	$[\eta]$ (100 cm³/g)	M.W. (kDa)[a]	Length (Å)[a]
Cod sperm	4.28	583	3050
Calf thymus	0.396	96	500
Salmon sperm	0.0445	26	140

a) The molecular weights are calculated from their intrinsic viscosities and the lengths are estimated using those values.

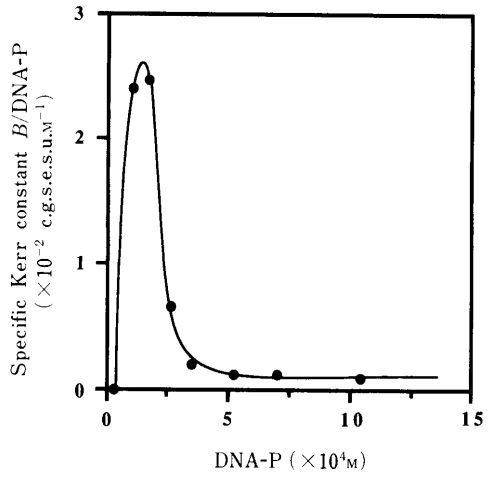

Fig. 5. Effect of Coralyne on the Specific Kerr Constant for DNA Solutions

Coralyne, 1.0×10^{-4} M.

To determine the apparent molecular weights of some DNAs, the viscosities were measured, and their molecular weights, M.W., were calculated from the intrinsic viscosity $[\eta]$ according to the equation[10]: $[\eta]=1.05\times10^{-7}$ M.W.$^{1.02}$. Table I shows the apparent molecular weights and lengths of cod sperm, calf thymus and salmon sperm DNAs. The molecular lengths were calculated using the mean molecular weight[10b] per nucleotide base-pair to be 650 Da and the distance between neighboring base-pairs to be 3.4 Å. In these DNA samples, cod sperm DNA was suitable for measurements of electric birefringence and ultrafiltration. Further viscosity measurements indicated that DNA molecules decay according to zero-order kinetics with a half-life of *ca.* 40 d at 4 °C. Therefore, we used cod sperm DNA solutions within seven days of their preparation.

Figures 5, 6 and 7 show the results obtained for the electric birefringence measurements of cod sperm DNA solutions, with and without coralyne. Figure 5 shows the

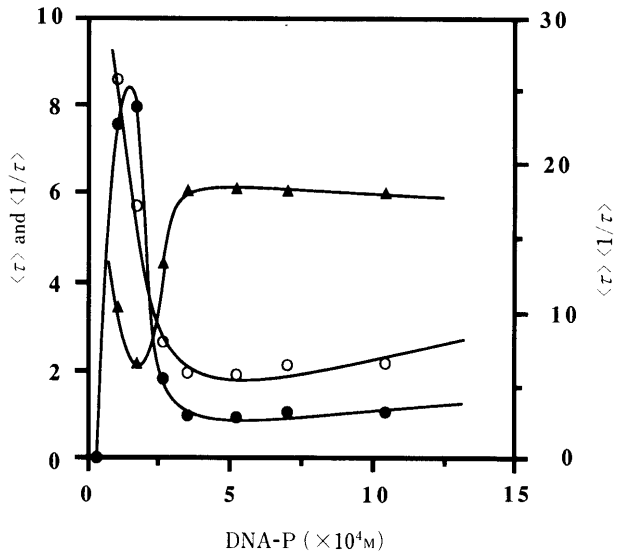

Fig. 6. Effect of Coralyne on the Mean Relaxation Times of DNA Solutions

Coralyne, 1.0×10^{-4}M; ●, mean relaxation time $\langle\tau\rangle$ in ms; ▲, reciprocal relaxation time $\langle 1/\tau\rangle$ in ms^{-1} and ○, their product $\langle\tau\rangle\langle 1/\tau\rangle$.

Table II. The Dimensions of the Aggregated Particles Estimated by the Mean Relaxation Times from Electric Birefringence Measurements

	DNA	DNA–coralyne complex	
		Type I	Type II
$\langle\tau\rangle_{biref}$ (ms)	0.59	7.95	1.0
Length (Å)	4000	4000	4000
Diameter (Å)	20	4000	120
$\langle 1/\tau\rangle_{biref}$ (ms^{-1})	17	2.1	6.10
Length (Å)	1700	1700	1700
Diameter (Å)	20	1400	200
$\langle 1/\tau\rangle_{biref}\cdot\langle\tau\rangle_{biref}$	10	17	8

effects of coralyne (1.0×10^{-4}M) on the specific Kerr constants at various DNA concentrations. This indicates that the critical aggregation of DNA with coralyne is maximum at near 2.0×10^{-4}M over the range 0.5—3.0×10^{-4}M DNA-P, *i.e.*, a coralyne to DNA-P ratio of 1 : 2, and then falls to that of DNA itself above this ratio. It is very interesting that such a critical aggregation is markedly enhanced only over a very narrow range, depending on the molar ratio. To obtain the actual dimensions of the aggregating particles, the decay curves were further analyzed using the initial slope (Eq. 6) and integration (Eq. 7) methods.[9] These results also showed that the aggregation is enhanced over a critical region of the molar ratio, as summarized in Fig. 6 and Table II. The particles are referred to as type I for the enhanced aggregation and type II for the others. Since the DNA molecule is assumed to be a rod-like particle with a diameter of 20 Å, its length was estimated to be 1700 and 4000 Å from $\langle 1/\tau\rangle_{biref}$ and $\langle\tau\rangle_{biref}$, respectively, using Eqs. 3 and 4. These values corresponded well with those estimated by viscosity. Now, one can assume that DNA molecules associate in a side-by-side manner only in solutions containing coralyne, and type I and II particles assume rotational prolate ellipsoid and a thick rod-like

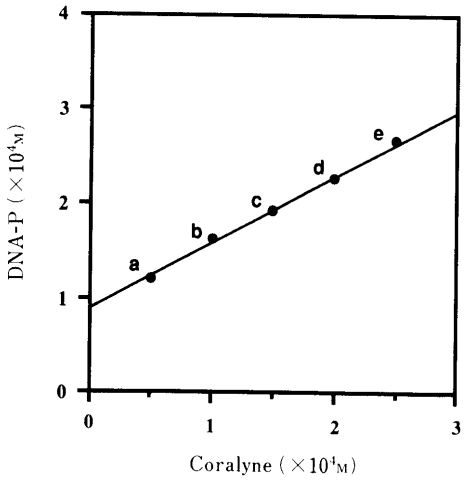

Fig. 7. Relationship between the Concentrations of DNA Phosphate ([DNA-P]) at $(B/C)_{max}$ and Coralyne (C)

The molar ratios of coralyne to DNA phosphate at $(B/C)_{max}$ were: a, 2.36; b, 1.58; c, 1.28; d, 1.11; e, 1.06; the solid line was calculated from the equation; $[\text{DNA-P}]=0.733C+0.821\times10^{-4}$.

shapes 1700—4000 Å in length, because of the values of their axis ratios. The lengths of those shorter axes were estimated to be 1400—4000 Å for type I, applying Eq. 5, and 120—200 Å for type II, applying Eq. 4. Therefore, type I and II particles may contain several tens of thousands and some hundreds of molecules of DNA, respectively. The distribution of particles in the three types of solutions should be similar, because the parameters for the multi-dispersion are similar, as shown in Fig. 6 and Table II. However, Fig. 7 indicates that the DNA aggregation also varies with the concentration (C) of coralyne. The concentration ([DNA-P]) of DNA phosphate at the maximum value $(B/C)_{max}$ of the specific Kerr constant was shifted by coralyne, according to a linear equation: $[\text{DNA-P}]=0.733C+0.821\times10^{-4}$. Since the equation did not pass through the origin, the molar ratio of DNA-P to one molecule of coralyne varied with the concentration of coralyne: a) 2.36, b) 1.58, c) 1.28, d) 1.11, e) 1.06. This suggests that the aggregation may be affected by a property of coralyne itself, *e.g.*, self-association.[11]

On the other hand, precipitation like from the DNA–coralyne solutions did not occur with any of the berberine–DNA solutions. The electric birefringence measurements did not show the occurrence of any enhanced critical aggregation (data not shown), and the berberine–DNA complex consisted of thick rod-like particles approximately 1700—4000 Å in length with a diameter of 300—1000 Å, over the observed region.

In order to obtain further information about the enhancement produced by coralyne and berberine, the interactions of coralyne and berberine with DNA were determined. Figure 8 shows a Scatchard plot for the interaction between coralyne and cod sperm DNA. The Scatchard plot indicates that the interaction is in a positive cooperative mode so that the binding reaction involves interaction between the binding sites and/or bound ligands. Such a cooperative interaction can be expressed by the Schwartz equation[12] (Eq. 10).

$$\frac{r}{C_f}=\frac{nK}{2}\left\{\frac{1}{KC_f}+\frac{1-1/KC_f}{\sqrt{4KC_f\sigma+(KC_f-1)^2}}\right\} \quad (10)$$

Where n, K and σ are binding parameters, r is the number of moles of bound coralyne per DNA-P, and C_f is the free coralyne concentration. The best fit of the binding curve gave $n=0.229\pm0.008$, $K=28.6\pm0.2\times10^4$, $\sigma=0.029\pm0.011$. This indicates that coralyne binds in the ratio of one molecule to *ca.* four DNA phosphate groups and that the interaction is a positive cooperative one, because the parameter σ is positive. The Scatchard plot further indicates that the interactive affinity becomes progressively stronger with the binding reaching a maximum at $r=0.18$, *i.e.* one molecule of coralyne binds with five DNA phosphate groups. However, above that ratio, the affinity becomes progressively weaker, because it involves nearest-neighbor ligand interactions. Davidson *et al.*[7a] have reported the binding between berberine and DNA in detail, but we measured the binding to obtain the parameters for our experiments. The interaction of berberine with DNA was demonstrated using the spectrophotometric method, and the Scatchard plot (Fig. 9) indicates that the interaction is a negative cooperative one or Langmuir-like.[13] Therefore, we analyzed it by applying the Langmuir equation (Eq. 11) and obtained $n_1=0.0476\pm0.0004$, $K_1=3.01\pm0.12\times10^4\,\mathrm{M}^{-1}$, $K_2=0.0766\pm0.0004\times10^2\,\mathrm{M}^{-1}$. This means that berberine binds in the ratio of one molecule of berberine to *ca.* ten DNA phosphate groups, which is less than that of coralyne.

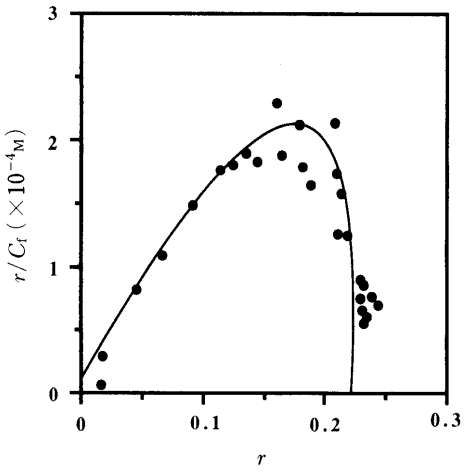

Fig. 8. Scatchard Plot for the Interaction between Coralyne and DNA

Cod sperm DNA phosphate, 0.95×10^{-4} M; coralyne chloride, 0—4.5×10^{-4} M.

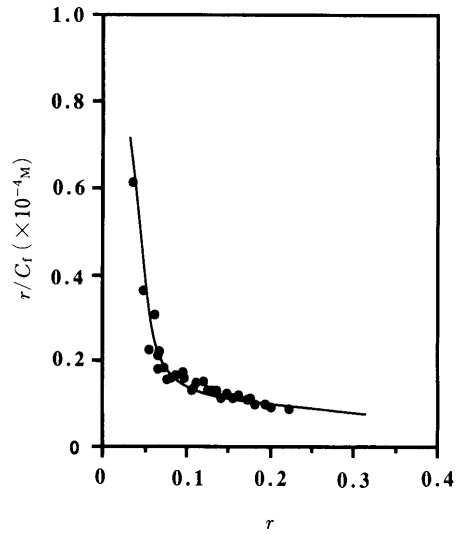

Fig. 9. Scatchard Plot for the Interaction between Berberine and DNA

Salmon sperm DNA phosphate, 0—40.5×10^{-3} M; berberine chloride, 1.0×10^{-3} M.

$$r=\frac{n_1K_1C_F}{1+K_1C_F}+K_2C_F \quad (11)$$

A Mechanism for Aggregation Zee-Cheng *et al.*[1a] have tried to interpret the aggregation of DNA by coralyne using the model of Bradley and Felsenfeld[6a] as mentioned above. However, the model could not account for the markedly enhanced aggregation of DNA by coralyne at the critical molar ratio, because the model does not reflect the variations in size of the aggregating particles. This may indicate that the aggregation is different from that of a dyestuff stacked along the DNA phosphate backbone, but similar to the precipitation of colloidal particles that takes place upon addition of ionic detergents. At present, the aggregation of colloidal particles is accounted for by the concept of bridging or mosaic forces between particles.[14] Figure 10 shows a modified model of the bridging concept in which the stacking interactions between coralyne molecules play a more important role in the aggregation. That is, since the negative net charges on DNA are neutralized by a positive charge on coralyne intercalated with the DNA or directly bound to phosphate

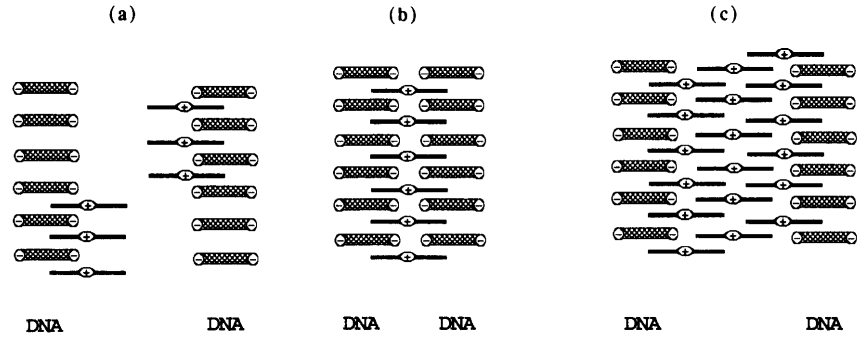

Fig. 10. A Proposed Model to Interpret the Enhanced Aggregation of DNA by Coralyne

(a) Intercalation of coralyne with DNA, (b) side-by-side assembly of DNA, (c) DNA assembly in the presence of excess coralyne.

(Fig. 10a), the DNA molecules may be more capable of aggregating (Fig. 10b). As the ratio of coralyne increases, those coralyne molecules stack together as well as stacking along the DNA phosphate backbone, *i.e.*, self-association,[11] and the particles are enlarged by side-by-side assembly in the molecular plane of coralyne protruding from the DNA (Fig. 10c). Those complexed DNA molecules should be aggregated by potent intercalation and/or ionic interactions. However, increasing coralyne does not result in enlarged particles but rather dissociation, because the attractive force between DNA molecules may be less potent. Therefore, precipitation occurs only over a critical range of DNA to coralyne ratio. The molecular structure of berberine is very similar to that of coralyne, except for the molecular planarity. Such a difference may be reflected in their aggregation: although berberine can intercalate into DNA as noted by Devidson *et al.*,[7a] it cannot precipitate DNA molecules, because berberine cannot stack around complexed DNA in a side-by-side manner.

How such an aggregation of DNA affects the course of DNA replication is a very interesting subject. However, we cannot account for it in detail at present and need to study it further.

References

1) *a*) K. Y. Zee-Cheng, K. D. Paull, C. C. Cheng, *J. Med. Chem.*, **17**, 347 (1974); *b*) R. K. Y. Zee-Cheng, C. C. Cheng, *ibid.*, **19**, 882 (1976); *c*) S. D. Phillips, R. N. Castle, *J. Heterocycl. Chem.*, **18**, 223 (1981).
2) *a*) M. L. Sethi, *J. Pharm. Sci.*, **72**, 538 (1983); *b*) *Idem*, *Phytochemistry*, **24**, 447 (1985); *c*) *Idem*, *J. Pharm. Sci.*, **74**, 889 (1985).
3) F. E. Hahn, A. K. Krey, *Progr. Mol. Subcell. Biol.*, **2**, 134 (1971).
4) *a*) M. Waring, *J. Mol. Biol.*, **54**, 247 (1970); *b*) E. J. Gabbay, D. Grier, R. E. Fingerle, R. Reimer, R. Levy, S. W. Pearce, W. D. Wilson, *Biochemistry*, **15**, 2062 (1976).
5) *a*) K. Y. Zee-Cheng, C. C. Cheng, *J. Pharm. Sci.*, **62**, 1752 (1973); *b*) W. D. Wilson, A. N. Gough, J. J. Doyle, M. W. Davidson, *J. Med. Chem.*, **19**, 1261 (1976); *c*) E. Smekal, J. Koudelka, *Studia Biophysica* (Berlin), **81**, 91 (1980).
6) *a*) D. F. Bradley, G. Felsenfeld, *Nature* (London), **184**, 1920 (1959); *b*) A. L. Stone, D. F. Bradley, *J. Am. Chem. Soc.*, **83**, 3627 (1961); *c*) J. Bontemps, E. Fredericq, *Biophys. Chem.*, **2**, 1 (1974).
7) *a*) M. W. Davidson, I. Lopp, S. Alexander, W. D. Wilson, *Nucleic Acids Res.*, **4**, 2697 (1977); *b*) A. Rungsitiyakorn, P. Wilairat, H. Panijpan, *J. Pharm. Pharmacol.*, **33**, 125 (1981); *c*) K. Yasukawa, M. Takido, T. Ikekawa, F. Shimada, M. Takeuchi, S. Nakagawa, *Chem. Pharm. Bull.*, **39**, 1462 (1991).
8) *a*) C. H. Fiske, Y. Subbarow, *J. Biol. Chem.*, **66**, 375 (1925); *b*) P. S. Chen, Jr., T. Y. Toribana, H. Warner, *Anal. Chem.*, **28**, 1756 (1956).
9) *a*) R. S. Wilkinson, G. B. Thurston, *Biopolymers*, **15**, 1555 (1976); *b*) M. Hogan, N. Dattagupta, D. M. Crothers, *Proc. Natl. Acad. U.S.A.*, **75**, 195 (1978); *c*) S. S. Wijmenga, A. Maxwell, *Biopolymers*, **25**, 2173 (1986); *d*) S. Broersma, *J. Chem. Phys.*, **32**, 1626 (1960); *d*) M. Matsumoto, H. Watanabe, K. Yoshioka, *Biopolymers*, **11**, 1711 (1972); *e*) K. Yoshioka, H. Watanabe, *Nippon Kagaku Zasshi*, **84**, 626 (1963); *f*) H. Sato, M. Shirai, *Progr. Colloid Polymer Sci.*, **68**, 138 (1983); *g*) J. B. Perrin, *J. Phys. Radium*, **5**, 497 (1934).
10) *a*) J. Eigner, P. Doty, *J. Mol. Biol.*, **12**, 549 (1965); *b*) W. J. Wood, J. H. Wilson, R. M. Benbow, L. E. Hood, "Biochemistry, a Problems Approach," 2nd ed., Benjamin/Cummings Pub. Co., Inc., California, 1981, p. 340.
11) A. N. Gough, R. L. Jones, W. D. Wilson, *J. Med. Chem.*, **22**, 1551 (1979).
12) G. Schwarz, *Biophys. Chem.*, **6**, 65 (1976).
13) *a*) Z. Taira, H. Terada, *Biochem. Pharmacol.*, **34**, 1999 (1985); *b*) A. R. Peacocke, J. N. H. Skerrett, *Trans. Faraday Soc.*, **52**, 261 (1956).
14) J. Gregory, *J. Colloid. Interface Sci.*, **42**, 448 (1973).